MOLECULAR ECOLOGY

Molecular Ecology (2016) **25**, 2093–2110 doi: 10.1111/mec.13597

Coexisting cryptic species of the *Litoditis marina* complex (Nematoda) show differential resource use and have distinct microbiomes with high intraspecific variability

S. DERYCKE,*† N. DE MEESTER,†‡ A. RIGAUX,†‡ S. CREER,§ H. BIK,¶ W. K. THOMAS** and T. MOENS§

*OD Taxonomy and Phylogeny, Royal Belgian Institute of Natural Sciences, Vautierstraat 29, 1000 Brussels, Belgium, †Department of Biology, Marine Biology Section, Ghent University, Krijgslaan 281 (S8), 9000 Ghent, Belgium, ‡CeMoFE, Ghent University, K.L. Ledeganckstraat 35, 9000 Ghent, Belgium, §Environment Centre Wales Building, School of Biological Sciences, Bangor University, Gwynedd LL57 2UW, UK, ¶Center for Genomics and Systems Biology, New York University, 12 Waverly Place, New York, NY 10003, USA, **Hubbard Center for Genome Studies, University of New Hampshire, 35 Colovos Road, 448 Greg Hall, Durham, NH 03824, USA

Abstract

Differences in resource use or in tolerances to abiotic conditions are often invoked as potential mechanisms underlying the sympatric distribution of cryptic species. Additionally, the microbiome can provide physiological adaptations of the host to environmental conditions. We determined the intra- and interspecific variability of the microbiomes of three cryptic nematode species of the *Litoditis marina* species complex that co-occur, but show differences in abiotic tolerances. Roche 454 pyrosequencing of the microbial 16S rRNA gene revealed distinct bacterial communities characterized by a substantial diversity (85–513 OTUs) and many rare OTUs. The core microbiome of each species contained only very few OTUs (2–6), and four OTUs were identified as potentially generating tolerance to abiotic conditions. A controlled experiment in which nematodes from two cryptic species (Pm1 and Pm3) were fed with either an *E. coli* suspension or a bacterial mix was performed, and the 16S rRNA gene was sequenced using the MiSeq technology. OTU richness was 10-fold higher compared to the 454 data set and ranged between 1118 and 7864. This experiment confirmed the existence of species-specific microbiomes, a core microbiome with few OTUs, and high interindividual variability. The offered food source affected the bacterial community and illustrated different feeding behaviour between the cryptic species, with Pm3 exhibiting a higher degree of selective feeding than Pm1. Morphologically similar species belonging to the same feeding guild (bacterivores) can thus have substantial differences in their associated microbiomes and feeding strategy, which in turn may have important ramifications for biodiversity–ecosystem functioning relationships.

Keywords: bacteria, coexistence, diet, individual niche specialization, marine nematodes, next-generation sequencing, resource partitioning, stabilizing effects

Received 24 June 2014; revision received 22 January 2016; accepted 12 February 2016

Introduction

Many taxa contain species that are morphologically (nearly) identical but show genetic differences in neutral markers that are comparable to, or greater than,

Correspondence: Dr. Sofie Derycke, Fax: +32 (0)2 627 41 41; E-mail: sofie.derycke@naturalsciences.be

those observed between species with distinct morphologies. These cryptic species have been observed in all major taxa and in all biogeographical regions (Pfenninger & Schwenk 2007). Despite their morphological similarity, cryptic species can have distinct evolutionary histories of millions of years (Elmer *et al.* 2013; Glasby *et al.* 2013; Perez-Portela *et al.* 2013). The conservation of the morphological pattern results from selection-promoting morphological stasis and/or from a differentiation in other characters that are invisible to the human eye (Bickford *et al.* 2007). In the marine environment, cryptic species of benthic invertebrates often show a sympatric distribution, but at the same time pronounced habitat preferences defined by depth, salinity, temperature and substrate (Knowlton 1993). Next to these abiotic parameters, intrinsic differences between cryptic species, such as the differential use of resources or the presence of distinct microbiomes, may impact the sympatric distribution of cryptic species as microbiomes can affect the physiology of the host (Cabreiro & Gems 2013; Sison-Mangus *et al.* 2014), which may have cascading effects on ecological interactions.

Substantial cryptic diversity has been observed in the phylum Nematoda (de Leon & Nadler 2010; Derycke *et al.* 2013; Ristau *et al.* 2013; Sudhaus & Kiontke 2007). In marine sediments, nematodes abound both in numbers and in local species diversity, with several tens of species co-occurring at submeter scales (Heip *et al.* 1985). Nematode community composition, assessed through morphological characters, can be linked to physicochemical characteristics of the sediment (Steyaert *et al.* 1999; Vanaverbeke *et al.* 2000), and at very small spatial scales, microhabitat differences can substantially alter nematode communities (Fonseca *et al.* 2010; Gingold *et al.* 2011). Based on the shape of the buccal cavity and the presence/absence of armature in the stoma, marine nematodes have been divided into feeding guilds (Moens & Vincx 1997; Wieser 1953). Nematodes without buccal armature can feed on bacteria and protists, while those having buccal armature can feed on microalgae (e.g. diatoms), on microinvertebrates including nematodes and on other resources (Moens & Vincx 1997). The niches of nematode species delineated by morphology are thus determined by a series of abiotic and biotic parameters, but the extent of niche breadth of, and niche differences between sympatrically occurring cryptic nematode species remain unknown. Moreover, the nematode microbiome influences the physiology of the worm and impacts its longevity (Cabreiro & Gems 2013) and may, especially in the case of bacterivorous nematodes, be linked to the diet of the nematodes. Techniques currently available to assess resource use in minute organisms (e.g. stable isotope analysis) are unable to distinguish individual resource use (Carman & Fry 2002). The advances in high throughput sequencing now allow to more deeply investigate the microbial communities associated with sympatric bacterivorous nematode species to determine the extent of resource differentiation (bacteria related to food) and of microbiome differentiation (the microbiome 'sensu lato', which comprises the bacteria related to food and the microbiome 'sensu stricto' containing the commensal bacteria).

The bacterivorous marine nematode *Litoditis marina* (Bastian, 1865) Sudhaus, 2011 consists of at least 10 cryptic species (Derycke *et al.* 2008b), three of which (Pm1, Pm2 and Pm3) frequently co-occur on seaweed stands and deposits in the coastal area of Belgium and the Netherlands (Derycke *et al.* 2005). In this region, the most abundant seaweeds typically belong to the genus *Fucus*. Phylogenetic analyses of mitochondrial and nuclear genes have revealed that Pm3 is more distantly related to Pm1 and Pm2 (Derycke *et al.* 2008b). Morphological differentiation between the three species is limited and requires a combination of morphometric characters (Derycke *et al.* 2008a). No cross-breeding between the species has been observed under laboratory conditions (Fonseca *et al.* 2008; Derycke, unpublished data). Their coexistence implies that local populations of the three sympatric species experience (nearly) identical sets of abiotic factors like salinity and temperature. Nevertheless, both factors differentially impact demographic traits of the three species, resulting in a significantly lower generation time at higher temperatures and the production of more offspring at lower salinities for Pm3 (De Meester *et al.* 2015b). Whether these species have a microbiome and whether such a microbiome would differ between species remains unknown. Furthermore, competitive interactions have been observed between these cryptic species (De Meester *et al.* 2011) and the presence of a bacterial food source impacted their dispersal behaviour (De Meester *et al.* 2012). In addition to abiotic factors, niche differentiation between the cryptic species may thus be linked to resource divergence. Chemotaxis and tracer experiments with the cryptic *L. marina* species and other bacterivorous nematodes have shown that they can selectively migrate towards and/or feed on bacterial strains (S. Derycke, personal observations; Estifanos *et al.* 2013; Moens *et al.* 1999). If such selective feeding is present in sympatrically distributed cryptic nematode species, this would support the idea that niche partitioning is an important process allowing their coexistence. Bacteria are the main food source of *L. marina*, but occasionally also small green algae are taken up (Moens & Vincx 1997). As such, *L. marina* is considered to be a deposit feeder (Moens & Vincx 1997). The oesophagus contains a distinct middle bulb and a

poorly developed posterior bulb with valves (Inglis & Coles 1961) which is very similar to the oesophagus of *C. elegans* and which grinds the bacteria before transmission to the intestine (Seymour *et al.* 1983). The microbiome 'sensu lato' may thus also be linked to feeding behaviour.

The aim of this study was to characterize the bacterial communities associated with co-occurring cryptic nematode species to reveal the extent of intra- and interspecific differentiation in the microbiome under natural field conditions. Single nematode specimens from each of three co-occurring species were simultaneously isolated from the same habitat in the same location, and a fragment of the microbial 16S rRNA gene was sequenced using the 454 GS FLX system (Roche). Next, to test whether the observed differences in bacterial communities are linked to resource use, we conducted a laboratory experiment with Pm1 and Pm3 nematodes which had been starved for 2 days before offering them *Escherichia coli* or a diverse bacterial mix. We expected to find significant differences in OTU composition between the two food treatments if the bacterial communities detected with the NGS approach indeed reflect resource use. Moreover, significant differences between species irrespective of food would indicate the presence of species-specific microbiomes, which may help explain their differences in abiotic tolerances (Cabreiro & Gems 2013).

Material and methods

Specimen collection

Individual nematode specimens have been collected in the framework of a geographical and seasonal investigation of the population genetic diversity in coastal and estuarine environments in Belgium and the southwest of the Netherlands in 2003 (Derycke *et al.* 2006). This study revealed that three closely related, cryptic *Litoditis* species (at that time *Pellioditis* marina) were co-occurring in the Paulina saltmarsh (51°21′N, 3°49′E) in October 2003 (Appendix S1, Supporting information). Fragments of living *Fucus* sp., one of the preferred habitats for *L. marina*, were randomly collected and incubated on agar slants (Moens & Vincx 1998). Nematodes were subsequently allowed to colonize the agar for about 2 days, during which they were able to feed on the natural bacteria associated with the *Fucus* fragments. No *E. coli* was added to these agar slants. After 2 days, specimens belonging to the *L. marina* species complex were identified under a dissecting microscope using diagnostic morphological characters (Inglis & Coles 1961) and handpicked from the agar with a fine needle. All worms were digitally photographed using light microscopy, and stored individually in 70–95% acetone until processed. Specimens were then assigned to cryptic species based on the COI genotyping from the population genetic survey (Derycke *et al.* 2006). We randomly selected six nematode specimens each of Pm1, Pm2 and Pm3 from the Paulina marsh samples.

DNA extraction and nematode identification

DNA was extracted using a simple lysis procedure by transferring individual nematodes to Worm Lysis Buffer (50 mM KCl, 10 mM Tris pH 8.3, 2.5 mM $MgCl_2$, 0.45% NP40, 0.45% Tween-20). The worms were then cut into pieces with a razor blade, frozen for 10 min at −20 °C and subjected to proteinase K (60 μg/mL) treatment. Finally, the DNA samples were centrifuged for 1 min at maximum speed (11 000 ***g***) and the supernatant was used in the subsequent PCR. In the original study, the mitochondrial cytochrome oxidase c subunit 1 (COI) gene was amplified and analysed using single-strand conformation polymorphism analysis (Derycke *et al.* 2006). To double-check species identity, we re-amplified and sequenced the COI gene of all specimens for which we still had sufficient DNA. PCR amplification was performed in 25 μL PCRs for 35 cycles, each consisting of a 30-s denaturation at 94 °C, 30-s annealing at 50 °C, and 30-s extension at 72 °C, with an initial denaturation step of 5 min at 94 °C and a final extension step of 5 min at 72 °C. Primers JB3 and JB5 were used (Derycke *et al.* 2006), and unidirectional Sanger sequencing was performed with JB3 by Macrogen. The obtained sequences were then compared to published sequences of the *L. marina* species complex (Derycke *et al.* 2008a). All samples used in this study had COI sequences that matched the SSCP-based identification.

16S rRNA gene amplification and 454 GS FLX sequencing of individual nematode specimens from the field

The bacterial communities associated with the six specimens from each of the three co-occurring nematode species Pm1, Pm2 and Pm3 were characterized through amplification of a portion of the 16S rRNA gene using the DNA extracts from the previous study. The 16S rRNA gene was amplified using primers 968F and 1401R (Zoetendal *et al.* 1998). Amplification was performed in 50 μL reactions containing 37.3 μL water, 5 μL buffer (10×), 1 μL dNTPs (10 mM each), 2 μL of each primer (10 μM) 0.2 μL TopTaq polymerase (Qiagen) and 2.5 μL DNA. Cycling conditions consisted of an initial denaturation of 2 min at 95 °C, followed by 35 cycles of 95 °C for 1 min, 53 °C for 45 s, 72 °C for 3 min, and a final extension of 72 °C for 10 min. The

number of cycles follows that of other environmental bacterial surveys (http://www.earthmicrobiome.org/emp-standard-protocols/16s/). The forward primer contained the Roche A adaptor (CGTATCGCCTC CCTCGCGCCATCAG) and an 11-bp MID tag, while the reverse primer contained the Roche B adaptor (CTATGCGCCTTGCCAGCCCGCTCAG) and an 11-bp MID tag. The MID tags are provided in Appendix S2 (Supporting information) and allowed separation of the sequences according to the nine nematode specimens. The resulting fragment was 505 bp long. A 'no template' control was included for each primer set to ensure no contamination occurred in the laboratory. PCR products were checked on 1% agarose gels, purified with AMPure beads following the manufacturer's protocol (Beckman Coulter Inc.) and measured with a Qubit fluorometer (Life Technologies). Samples were then pooled in equimolar concentrations and loaded on the Bioanalyzer (Agilent Technologies) to check the presence of a single peak. The pooled sample was bidirectionally sequenced on 1/8 of a 454 GS FLX plate (Macrogen). Two runs were performed, each containing three specimens from each species.

Data analysis

The raw data sets from the two runs were filtered and denoised with FlowClus (Gaspar & Thomas 2015), a program that uses the flow information in the sff.file to screen and correct errors. FlowClus is available for downloading at http://sourceforge.net/projects/flowclus/. Primers and barcodes were removed from the sequences, and the reverse complement was taken of the reverse sequences. Filtering involved removal of sequences that were outside the 200–1000 bp range, had an average quality <25, or contained more than six homopolymers. Denoising was chosen with a constant value of 0.5. Chimera's were detected using UCHIME without reference database (Edgar *et al.* 2011) and removed from the data set. The sequences were then processed using QIIME 1.9.0 (Caporaso *et al.* 2010). Forward sequences from both runs were merged to create a data set with only forward sequences. The reverse sequences from both runs were also merged to create a data set with only reverse sequences. Unlike for the paired-end reads generated with Illumina, the forward and reverse data sets generated by the 454 protocol cannot be merged because forward and reverse reads are not generated from the same PCR molecule. Therefore, the resulting forward and reverse data sets were independently clustered into OTUs with 97% similarity using an open-reference OTU picking strategy. OTUs that were only observed once in the total data set were removed because these are most likely to represent sequencing errors or rare variants within genomes. Default settings of QIIME 1.9.0 were used, except for the subsampling in the open-reference OTU picking strategy, which was set at 0.01 instead of 0.001. The number of sequences and OTUs obtained for each of the 18 specimens is summarized in Appendix S3 in Supporting Information.

Taxonomy was assigned up to species level using the assign_taxonomy.py script and the 97% taxonomy and OTU files of the Greengenes 13.8 database, using the default settings of the Uclust algorithm as implemented in QIIME. When no hit was observed, OTUs were labelled as 'Unassigned'. The taxonomic compositions associated with each of the three nematode species were visualized through bar graphs in excel using the unrarefied data set for both F and R data sets.

Diversity within and between the three cryptic species was compared. To account for differences in number of sequences for each specimen, the data set was rarefied at 600 sequences per specimen for each data set. This number was slightly lower than the lowest number observed in our samples (626 for the forward data set, 643 for the reverse data set; see Appendix S1, Supporting information). Alpha diversity (Shannon-Wiener, observed OTUs, Good's coverage) was calculated using alpha_rarefaction.py in QIIME. Rank abundance graphs were constructed to explore the abundance of OTUs associated with each nematode specimen. Generalized UniFrac distances ($\alpha = 0.05$) (Chen *et al.* 2012) were calculated with the GUniFrac package in R (Team 2008). PERMANOVA was conducted on these UniFrac distances with species as grouping variable using the Adonis package in R. PERMDISP and pairwise difference tests were also performed in R. Principal coordinates analysis (PCoA) plots were generated to visualize intra- and interspecific differences between the treatments using the Ade4 package in R. In addition, we investigated whether differences between species were caused by differences in rare OTUs, by constructing a data set with only those OTUs that had at least 108 sequences (i.e. 1% of the rarefied data set, which contained 18*600 = 10 800 sequences). This resulted in a forward and reverse data set containing 18 OTUs with a frequency higher than 1%. Statistical analyses on these data sets were performed as described above.

To investigate whether each of the nematode species had bacterial OTUs that were present in all specimens of that particular species (=the core microbiome of each species), we ran the compute_core_microbiome.py script. The frequency of the core OTUs in each specimen was visualized using the sequence counts from the rarefied biom table. Because many bacterial strains show a lower than 3% divergence, we investigated whether the core community would be impacted by

clustering OTUs at 99% instead of 97%. For this, we reran the open-reference OTU picking strategy for the reverse data set using a similarity of 99%. Taxonomic assignment was performed using the 99% taxonomy and OTU files of the Greengenes 13.8 database. All other settings and parameters and core microbiome analysis were identical as mentioned above.

Biomarker taxa that are most likely to explain differences in microbiome between the three nematode species were assessed using the Linear discriminant analysis Effect Size (Segata *et al.* 2011) module as implemented in Galaxy (https://huttenhower.sph.harvard.edu/galaxy). Default settings were used, and species were selected as class and specimens as subjects. We used the rarefied reverse data set clustered at 97%.

Food experiment

To investigate whether the bacterial communities associated with the nematodes were part of the diet, living worms of Pm1 and Pm3 were subjected to two different food treatments: an *E. coli* treatment (Pm1E and Pm3E) and a 'bacterial mixture' treatment (Pm1B and Pm3B) in which nematodes were fed a natural inoculum of bacteria from the field. Fragments of the seaweed *Fucus* sp. from Paulina were put in culture flasks with artificial sea water (ASW) with a salinity of 25 for 1 week at a temperature of 15 °C and afterwards rinsed in ASW with a salinity of 25. The ASW from the culture flasks and the washing step was filtered three times over a GF/C filter with a diameter of 1.2 μm to remove organisms with sizes exceeding those of bacteria, and frozen at −20 °C until the experiment started. Two times 5 μL of this suspension was used for DNA extraction for later bacterial-diversity analysis ('bacterial mixture'). Four Petri dishes of 5 cm inner diameter were filled with 4 mL of 1% bacto agar medium (salinity of 25 and buffered at a pH of 7.5–8 with Tris–HCl in a final concentration of 5 mM). Two dishes received 50 μL of a suspension of frozen-and-thawed *E. coli* (strain K12 in PBS buffer) with a density of 3×10^9 cells/mL to which either 20 adult Pm1 or 20 adult Pm3 nematodes were added. The two remaining dishes received 50 μL of the bacterial mix prepared from the *Fucus* thalli to which either 20 adult Pm1 or Pm3 nematodes were added. Monospecific cultures of the two cryptic species were raised from one single gravid female per species collected from Paulina marsh (the Netherlands) in March 2014 and maintained on sloppy (0.8%) nutrient:bacto agar media (temperature of 20 °C; salinity of 25) with unidentified bacteria from their habitat as food (Moens & Vincx 1998). Two pieces of agar of each nematode culture (Pm1 and Pm3) were subjected to a DNA extraction and 16S rRNA gene amplification to pinpoint the bacteria that are able to grow on the culture medium. Nematodes were allowed to feed on the bacteria for 2 days, after which ten nematodes per treatment were picked out and quickly washed in cold sterile ASW to remove most of the adherent bacteria. Subsequently, they were put individually in 20 μL WLB for DNA extraction. The DNA extraction was the same as described for the field specimens. For the pure bacterial mixture a DNA clean-up (Wizard) was necessary after the DNA extraction, due to the high salt concentration in the solution. In total, 46 DNA extracts were prepared (10 for each of the four food treatments, 2 from the agar from each stock culture, and 2 from the bacterial mixture).

16S rRNA amplification and Illumina MiSeq sequencing of individual nematode specimens from the food experiment

For the DNA amplification and Illumina MiSeq sequencing, a slightly adapted version of the protocol of the Earth Microbiome Project (Gilbert *et al.* 2014) was used. Amplification was performed in 20 μL reactions containing 11.4 μL water, 4 μL 10× buffer, 0.4 μL dNTP's (10 mM), 0.2 μL Phusion (high-fidelity) polymerase, 2 μL DNA template and l μL forward and 1 μL reverse primer (both 10 μM). The forward primer contained the 5′ Illumina adaptor, forward primer pad and linker and the 515f primer. The reverse primer consisted of the reverse complement of the 3′ Illumina adapter, the reverse primer pad and linker, the 806r primer and a Golay barcode. This Golay barcode was unique for each sample, and the first 52 barcodes of the Earth Microbiome Project were used (Caporaso *et al.* 2012). Cycling conditions consisted of an initial denaturation of 30 s at 98 °C, followed by 35 cycles of 98 °C for 10 s, 65 °C for 30 s, 72 °C for 15 s, and a final extension of 72 °C for 10 min. Samples were amplified in triplicate. Three samples were randomly chosen in which the triplicates received different barcodes to allow investigation of PCR cycle bias. We did detect some PCR bias, but most OTUs were shared between replicas and OTUs uniquely found in one replica reached only very low frequencies (maximum of 0.21%). All analyses regarding the technical replicates can be found in Appendix S4 (Supporting information). After amplification, triplicates were combined. PCR products were cleaned by selecting the correctly sized bands (300–350 bp) with the help of CloneWell Agarose Gels (E-Gel). After this, the PCR concentration was measured with the Qubit Fluorometer (Life Technologies) and an equal amount of amplicon from each sample was pooled into one single, sterile tube. The final

sample was checked for concentration and quality with the Bioanalyzer (Agilent Technologies). Illumina MiSeq sequencing was performed by the Genomics Core (UZ Leuven). Because only a small amount of reads from the nematodes fed *E. coli* were assigned to Enterobacteriaceae (see results), the *E. coli* suspension was sequenced in a separate MiSeq run (as part of a follow-up experiment) to exclude any methodological issues. Three biological replicas of the suspension were amplified and sequenced as described above.

Data analysis

The Illumina paired-end sequences were first assembled with PEAR (Paired-End reAd mergeR; Zhang *et al.* 2014). Subsequent filtering involved trimming of reads with a quality score of 25, read lengths had to be in the 200–1000 bp range, and all reads containing uncalled bases were discarded. Subsequently, forward and reverse primers were removed with Cutadapt (Martin 2011). The sequences were then processed using QIIME 1.8.0 (Caporaso *et al.* 2010) with an open-reference OTU picking strategy (97% clustering) as described above. Beta-diversity analyses involved rarefaction of the data set at 41 000 sequences for each sample. Generalized UniFrac distances ($\alpha = 0.05$) (Chen *et al.* 2012) were calculated and statistical analyses were conducted in R as described above. The technical replicates that received a different barcode to investigate PCR bias were merged into a single sample for alpha- and beta-diversity analyses. The rarefied data set was also used to identify biomarker taxa between Pm1 and Pm3 related to resource use using species as class, food treatment as subclass and specimens as subjects. Default settings were used.

The *E. coli* samples were separately analysed from the first MiSeq run, but the same assemblage, filtering, trimming, OTU clustering and taxonomic assignment procedures were used.

Scanning electron microscopy (SEM)

In our previous study, all specimens were photographed digitally prior to the DNA extraction to have a morphological reference before being stored in acetone. To assess the abundance of bacteria associated with the nematode cuticle, we re-examined the digital pictures of the specimens used for next-generation sequencing. In addition, nematodes grown on agar media with unidentified bacteria from their habitat and *E. coli* as additional food, from monospecific cultures of each of the three nematode species were used to generate SEM pictures of the head, tail and midbody region. These SEM pictures were generated to investigate the abundance and diversity of bacteria on the cuticle of the nematodes. The numbers of females photographed were 7, 3 and 7 for Pm1, Pm2 and Pm3, respectively, and the numbers of males were 9, 4 and 3, respectively. SEM pictures were generated with the JEOL JSM-840 scanning electron microscope by the Nematology Unit of the Biology Department at Ghent University.

Results

16S rRNA composition of individual nematode specimens from the field

Taxonomic composition of the bacterial communities associated with cryptic species. Taxonomic assignments at the phylum level were highly comparable for the forward and reverse data sets and only differed in the presence of an additional three 'phyla' ('unidentified bacteria', Planctomycetes and 'TM6') in very low frequency in the reverse data set. We restrict the detailed description of the taxonomic composition to the reverse data set, because it yielded slightly more sequences for each sample (Appendix S3, Supporting information). Taxonomic composition at the phylum level for the forward data set can be found in Appendix S5 (Supporting information).

The microbiomes of all three nematode species were dominated by the phylum Proteobacteria (53%, 70% and 73% for Pm1, Pm2 and Pm3, respectively). The phyla Bacteroidetes (10%, 14% and 1.8% for Pm1, Pm2 and Pm3, respectively) and Actinobacteria (17%, 6% and 5% for Pm1, Pm2 and Pm3, respectively) were the second and third most abundant group of bacteria, which were found in nearly all specimens (17 and 18 of the specimens, respectively). The Verrucomicrobia were present in 5 of the 6 specimens of Pm3 with an average relative frequency of 16%, whereas its frequency in Pm1 and Pm2 was <1% and 4%, respectively, and in 4 and 2 of the 6 specimens, respectively. The Firmicutes group was present in all 18 specimens in similar frequencies (2.1%, 3.6% and 3.8% in species Pm1, Pm2 and Pm3, respectively). In total, 79 OTUs were unassigned, but nearly all of them had a relative frequency of <1% and their total abundance reached 9.9%. New.ReferenceOTU30 was prominent in Pm1 (12% in the rarefied data set), but only in one replicate. Within the phylum Proteobacteria, the Gammaproteobacteria dominated the microbiomes of Pm1 (82.7%) and Pm2 (72.7%) and to a lesser extent the microbiome of Pm3 (46.4%) (Fig. 1A) and contained 57 taxa from 22 known families (Fig. 1B). The Alteromonadaceae and Moraxellaceae were among the most abundant families shared between the three species and were especially abundant in Pm3 (12.6% and 15.5%) (Fig. 1B). The Alphaproteobacteria formed the second most abundant class within the Proteobacteria and represented 9.6%, 18.1% and 44.2% of the assigned

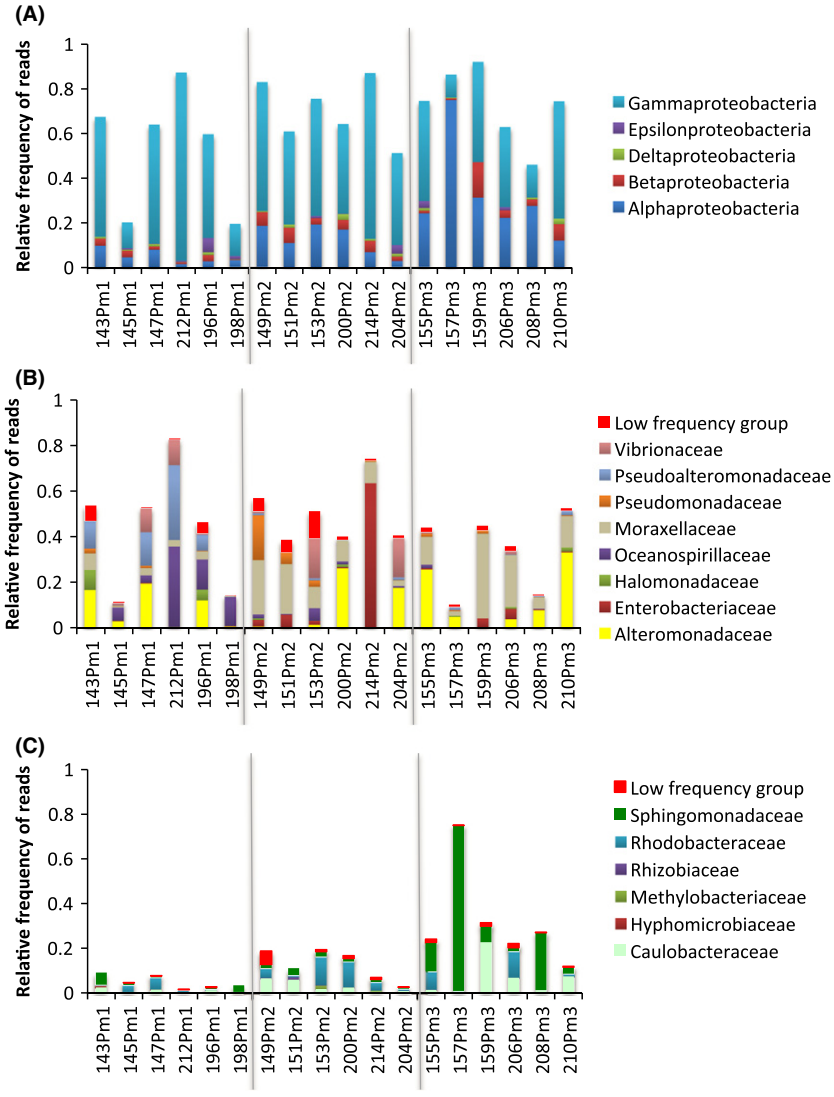

Fig. 1 Relative composition of Proteobacteria for each of the 18 nematode specimens. Reads are from the reverse data set. (A) Class-level and (B) family-level Gammaproteobacteria; the eight most abundant taxa are shown, and the 14 remaining taxa are pooled in a 'Low Frequency Group'; (C) Family-level Alphaproteobacteria; the six most abundant taxa are shown, and the nine remaining taxa are pooled in a 'Low Frequency Group'. Vertical grey lines denotes grouping of specimens according to species Pm1, Pm2 and Pm3.

taxa of Pm1, Pm2 and Pm3, respectively (Fig. 1A). This group comprised 44 taxa belonging to 15 known families, of which the Caulobacteraceae, Rhodobacteraceae and Sphingomonadaceae were the most abundant (Fig. 1C). In particular, the latter family was much more abundant in Pm3 (20.7%) than in Pm1 (1.8%) and Pm2 (1.7%) but this was caused by a high abundance in one specimen (175Pm3; Fig. 1C). The Beta, Delta and Epsilon Proteobacteria were only poorly represented, and contained 28, 10 and 2 taxa, respectively.

Within the phylum Actinobacteria, more than 99% of the taxa belonged to the Actinobacteria class, within which 17 families were assigned (Fig. 2A). Two families, the Corynebacteriaceae and the Microbacteriaceae, were prominent in all three nematode species. The high abundance of the Microbacteriaceae in Pm1 was mainly caused by a high abundance in a single specimen (145Pm1; Fig. 2A).

Within the phylum Bacteroidetes, two classes encompassed more than 99% of the assigned taxa: the Flavobacteria dominated Pm1 and Pm3 (75.3% and 81.8%, respectively), while the Cytophagia dominated Pm2 (68.0%, vs. 23.2% and 17.4% in Pm1 and Pm3). Both classes were represented by only two families: the Cytophagia consisted of Cytophagaceae and Flammeavirgaceae (Fig. 2B), the latter being found in very low abundance and in only one specimen of each species; the Flavobacteria consisted of Flavobacteriaceae, Cryomorphaceae and Weeksellaceae, the former being dominant in Pm1, while the Weeksellaceae were abundant in Pm2 (Fig. 2B).

Alpha diversity of field specimens. Rarefaction curves of the number of observed OTUs yielded highly similar results for forward and reverse data sets. Curves were still increasing at a sampling depth of 600 sequences

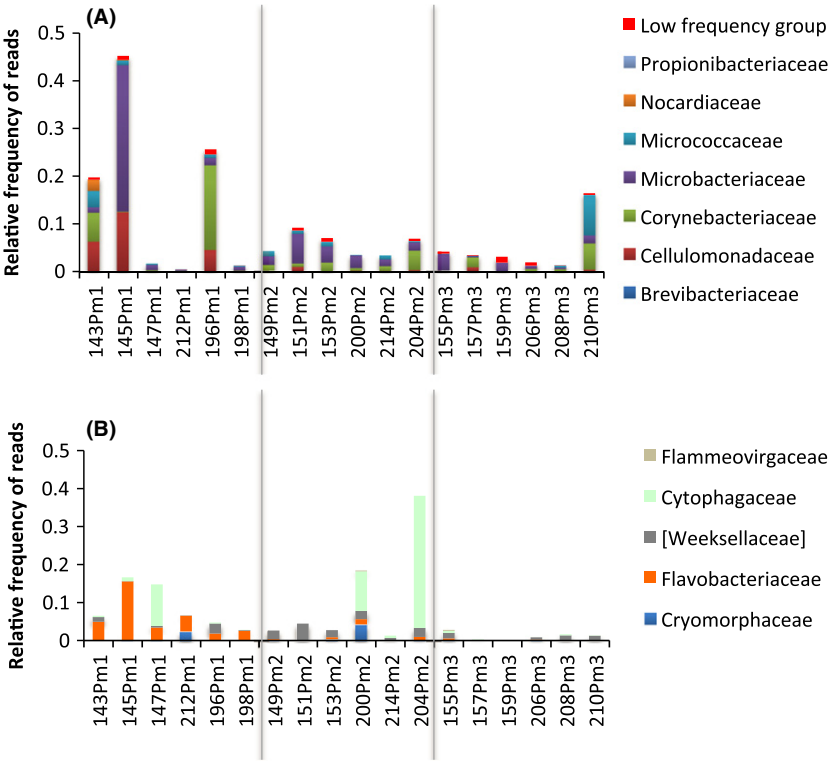

Fig. 2 Relative taxonomic composition of bacteria for each nematode specimen at the family level. Reads are from the reverse data set. (A) Actinobacteria, the seven most abundant families are shown, the remaining ten families are pooled in a 'Low Frequency Group'. (B) Bacteroidetes. Vertical grey lines denotes grouping of specimens according to species Pm1, Pm2 and Pm3.

per nematode specimen (Fig. 3A, Appendix S5, Supporting information). In contrast, the Shannon diversity measure quickly reached a plateau (Fig. 3B, Appendix S5, Supporting information), suggesting that many OTUs occur in very low frequencies. This was confirmed by the rank abundance plot, which illustrates that only a few OTUs have relative abundances higher than 0.1, while many OTUs have very low relative abundances (Appendix S6, Supporting information).

Beta diversity of field specimens. PERMANOVA based on the Generalized UniFrac distances showed significant differences between the microbial communities of the nematode species for both forward and reverse data sets and with or without inclusion of rare OTUs (Table 1). Post hoc tests revealed that these differences were situated between Pm1 and Pm3, regardless of the data set used. The six specimens within species did, however, show substantial variability (Fig. 4, Appendix S5, Supporting information). The nonsignificant PERMDISP results (Table 1) indicated that intraspecific differences were comparable for each of the three species.

The core microbiome of field specimens. Despite the high number of OTUs observed for each nematode species (see Appendix S3, Supporting information), none of them were shared between all 18 specimens. The core microbial community for each species consisted of very few OTUs (5, 5 and 2 OTUs for species Pm1, Pm2 and Pm3 in the forward data set, respectively, and 5, 6 and 4 OTUs for species Pm1, Pm2 and Pm3 in the reverse data set, respectively; see Appendix S7, Supporting information). Frequencies of the core communities were overall low in each of the 18 specimens, but 4 and 6 core OTUs of the forward and reverse data sets, respectively, reached frequencies higher than 1% (Fig. 5). The core communities of species Pm1 and Pm2 were also present in the other species, while the core community of species Pm3 was nearly absent in the two other species. PERMANOVA on the generalized UniFrac distances yielded only borderline (non)significant differences between the three species (reverse data set: $F = 2.40$, $P = 0.058$; forward data set: $F = 2.94$, $P = 0.048$), suggesting that the core communities were phylogenetically similar to each other. Small differences in taxonomic composition were however present (Appendix S7, Supporting information). OTU clustering at 99% slightly increased the number of core OTUs (8 vs. 5 for Pm1, 6 vs. 6 for Pm2 and 5 vs. 4 for Pm3) which was mainly due to an increase of OTUs identified as Moraxellaceae. Taxonomic composition was very similar to that observed with 97% clustering (Appendix S7, Supporting information).

Biomarker taxa of the field specimens. The LeFSe analysis indicated 1, 2 and 6 taxa that significantly differentiated Pm1, Pm2 and Pm3, respectively, and with an LDA score higher than two. The biomarker for Pm1 belongs to the genus *Pseudoalteromonas* (OTU4406967). New.Refer-

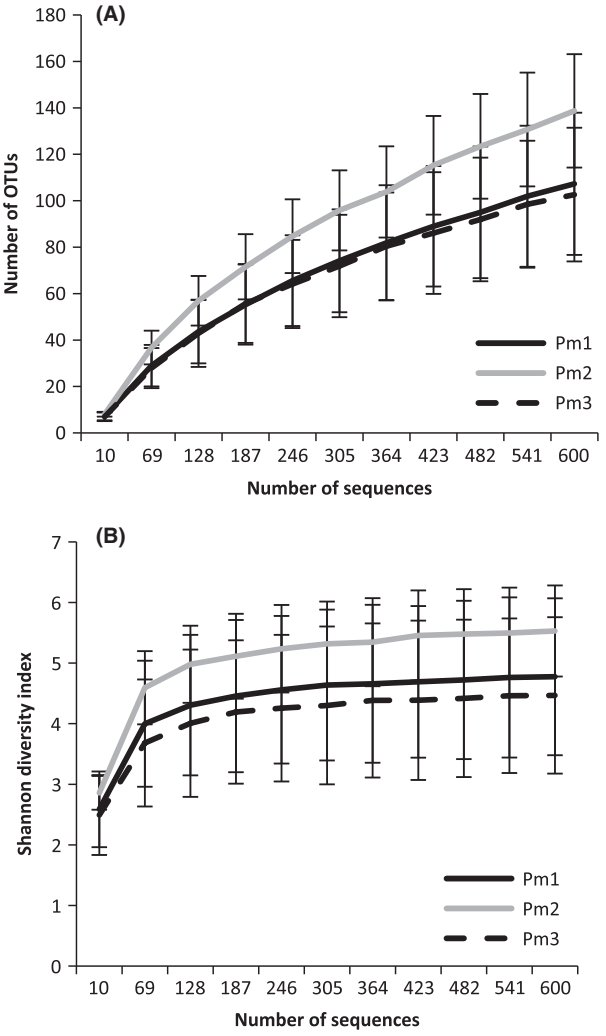

Fig. 3 Rarefaction curves of the number of observed OTUs at 97% sequence identity clustering (A) and Shannon index (B) for each species for the reverse data set. Error bars were calculated from the variance of the respective parameter drawn in 10 randomizations at each sample size.

enceOTU37 and OTU200979 were identified as biomarker for Pm2 and belong to the genus *Microbacterium* and the ordo Saprospirales, respectively. The biomarker taxa of Pm3 were identified as Verrucomicrobiaceae (New.ReferenceOTU54 and OTU4307243), *Acinetobacter* (OTU4449456), Moraxellaceae (OTU4334053), Caulobacteraceae (OTU310003) and Comamonadaceae (OTU115161) (Appendix S7, Supporting information).

16S rRNA composition of individual nematode specimens from the food experiment

To investigate whether the observed differences in the microbiomes of Pm1 and Pm3 were related to selective feeding, we performed a food experiment in which both species were offered *E. coli* or a diverse bacterial mix as food. The MiSeq protocol generated a much larger number of sequences and OTUs per nematode specimen (Appendix S8, Supporting information) than the 454 protocol. A detailed description of the taxonomic composition of the nonrarefied data set of the food experiment can be found in Appendix S9 (Supporting information). The microbiomes of all samples were clearly dominated by Proteobacteria and Bacteroidetes (Fig. 1 in Appendix S9, Supporting information). At the family level, the microbiomes of the two food treatments showed some striking differences between each other, but also between species: (i) within Alphaproteobacteria, the microbiomes of Pm3 worms fed the bacterial mixture resembled the bacterial mixture, while the microbiomes of the Pm3 worms fed *E. coli* contained a substantial amount of Rhodobacteraceae, which were highly abundant in the Pm3 stock cultures (Fig. 6A). In contrast, Pm1 worms showed very similar compositions regardless of the offered food. (ii) Within Gammaproteobacteria, the microbiomes of Pm1 and Pm3 fed the bacterial mix were similar to that of the bacterial mix. The microbiomes of Pm1 and Pm3 worms fed *E. coli* resembled that of the stock cultures of each species (Fig. 6A). Surprisingly, the worms fed *E. coli* were not enriched for Enterobacteriaceae. However, the *E. coli* suspension that was offered to the nematodes in the *E. coli* treatments was dominated by Enterobacteriaceae (Fig. 6B). (3) Within the Bacteroidetes, all Pm3 worms were dominated by Saprospiraceae, the

Table 1 Summary of the PERMDISP and PERMANOVA statistics between the microbiomes of the nematode species Pm1, Pm2 and Pm3. Analyses were carried out on the forward and reverse data sets using all OTUs or only those OTUs with relative frequency in the rarefied data set ≥1%. For the pairwise comparisons, significant *P*-values after Bonferroni correction are indicated in bold.

		All OTUs		OTUs > 1%	
		F	*P* value	*F*	*P* value
Forward data set					
PERMDISP		0.51	0.61	0.75	0.49
PERMANOVA		1.79	0.007	1.76	0.04
Pairwise test	Pm1-Pm2	1.55	0.03	1.34	0.19
Pairwise test	Pm1-Pm3	2.21	**0.008**	2.65	**0.016**
Pairwise test	Pm2-Pm3	1.61	0.062	1.37	0.23
Reverse data set					
PERMDISP		1.73	0.211	1.69	0.22
PERMANOVA		1.62	0.001	1.90	0.012
Pairwise test	Pm1-Pm2	1.40	0.032	1.46	0.11
Pairwise test	Pm1-Pm3	2.11	**0.002**	2.88	**0.004**
Pairwise test	Pm2-Pm3	1.36	0.074	1.50	0.13

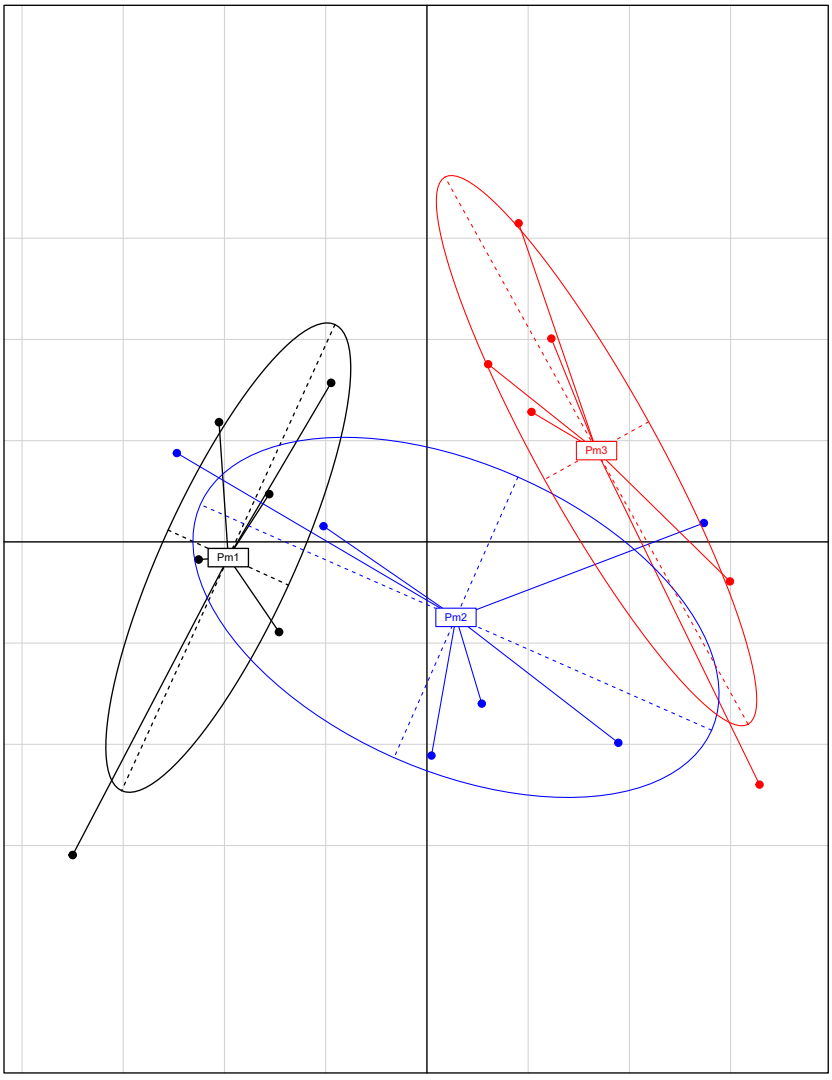

Fig. 4 Principal coordinates analysis plot based on generalized UniFrac distances between 18 nematode specimens after rarefaction at 600 sequences per specimen of the reverse data set from the 454 platform. Intraspecific distances for Pm1 (black), Pm2 (blue) and Pm3 (red) are encircled.

dominant family of the bacterial mix. Abundances of this family were higher in the Pm3 worms fed the bacterial mix than those that had been fed *E. coli*. For Pm1, taxonomic composition of both food treatments was comparable (Fig. 6A).

Alpha diversity of specimens from the food experiment. The average number of OTUs observed in the nematodes fed the bacterial mix was similar to that in those fed *E. coli* (Kruskal–Wallis: df = 6, $P = 0.08$). Patterns of species diversity and richness were very similar to the data on the field specimens: the number of OTUs was still increasing at a sampling depth of 41 000 sequences per treatment, the Shannon diversity measure quickly reached a plateau, and the rank abundance plots again show that many OTUs have very low relative abundances (Appendix S9, Supporting information). Four OTUs were highly abundant in the Pm1 specimens from the *E. coli* treatment and are thus likely to be part of the microbiome sensu stricto: *Pseudoalteromonas* (ca 98 000 reads), *Agrobacterium* (ca 69 000 reads), Unassigned (ca 57 000 reads) and *Winogradskyella thalassocola* (ca 32 000 reads). When blasted in GenBank, the unidentified OTU was most similar to an uncultured bacteria from a water cave (accession no. FJ604748.1). The most highly abundant Pm3E OTU (ca 150 000 reads) was the same unidentified OTU as for Pm1E.

Beta diversity of specimens from the food experiment. PERMANOVA based on the generalized UniFrac distances of the four food x species treatments (Pm1B, Pm1E, Pm3B, Pm3E) showed significant differences between food (pseudo-$F_{1.39} = 3.42$; $P = 0.005$) and species (pseudo-$F_{1.39} = 10.97$; $P = 0.001$). The interaction between food and species was only just significant (pseudo-$F_{1.39} = 2.02$; $P = 0.049$). Pairwise comparisons were all significant,

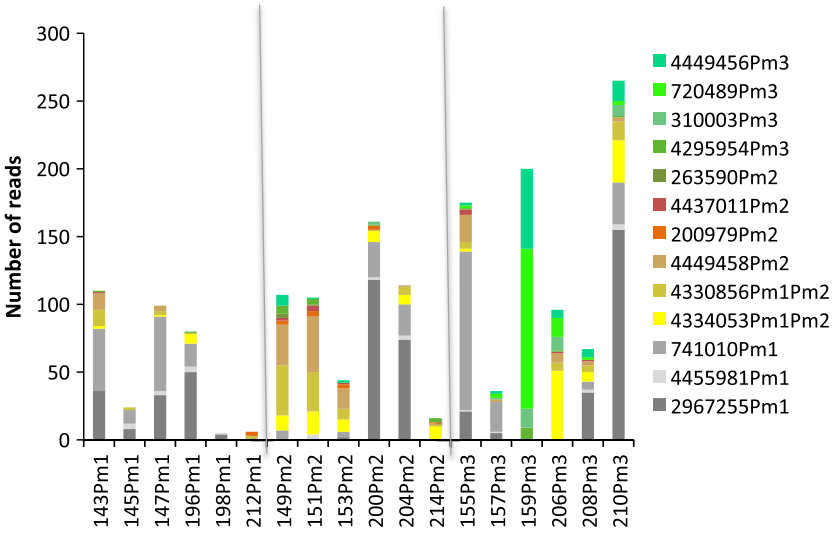

Fig. 5 Number of reads assigned to the core OTUs of Pm1, Pm2 and Pm3 in each of the 18 specimens from the rarefied reverse data set. Legend reflects OTU name followed by the name of the species in which they were the core (e.g. 4334053Pm1Pm2 indicates that OTU 4334053 was present in all six specimens of Pm1 and in all six specimens of Pm2). Vertical grey lines denotes grouping of specimens according to species Pm1, Pm2 and Pm3.

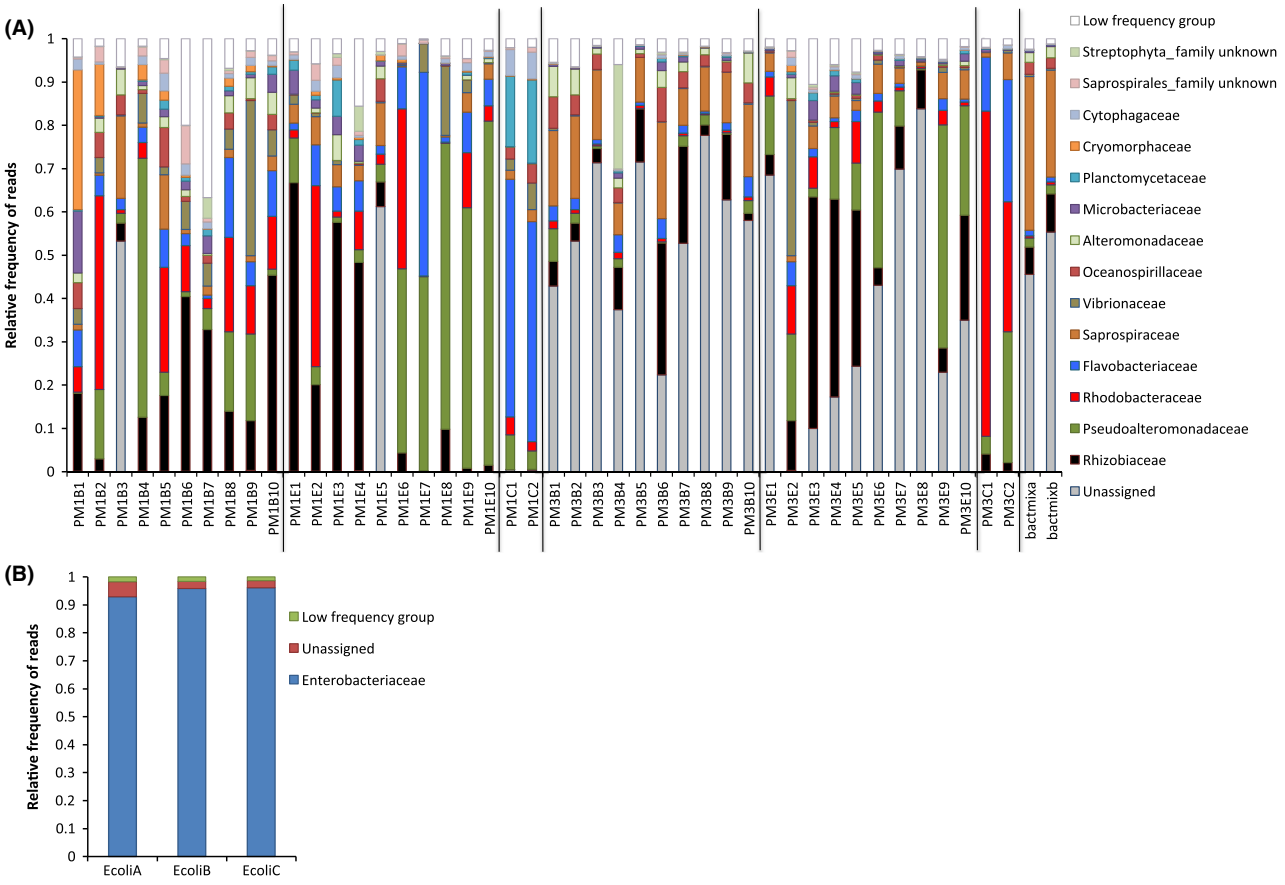

Fig. 6 Taxonomic assignment of MiSeq reads at the family level for (A) the food experiment and (B) three biological replicas of the *E. coli* suspension. For the food experiment, the 15 most abundant families are shown, the remaining families are pooled in a 'Low Frequency Group'. Pm1B1-10: 10 biological replicas of Pm1 fed the bacterial mixture; Pm1E1-10: 10 biological replicas of Pm1 fed *E. coli*; Pm1C1-2: two biological replicas of the agar from Pm1 stock cultures; Pm3B1-10: 10 biological replicas of Pm3 fed the bacterial mixture; Pm3E1-10: 10 biological replicas of Pm3 fed *E. coli*; Pm3C1-2: two biological replicas of the agar from Pm3 stock cultures; bactmixa-b: two biological replicas of the bacterial mix. Vertical grey lines denote the different food treatments, stock cultures and bacterial mix. EcoliA–EcoliC: three biological replicas of the *E. coli* suspension. The 'Low Frequency Group' contains 16 families.

Table 2 Summary of the PERMDISP and PERMANOVA statistics between the microbiomes of the four food experiment treatments (Pm1B, Pm1E, Pm3B and Pm3E) for the data set containing all OTUs and for the core OTUs. For the pairwise comparisons, significant *P*-values after Bonferroni correction are indicated in bold.

		All OTUs		Core Genome	
Food experiment		Pseudo-*F*	*P* value	Pseudo-*F*	*P* value
PERMDISP	Species	9.04	<0.001	7.11	0.011
	Food	2.94	0.095	1.57	0.22
	Species*food	6.80	<0.001	6.65	0.001
PERMANOVA	Species	10.97	0.001	16.56	0.001
	Food	3.10	0.005	3.59	0.008
	Species*food	2.02	0.049	2.46	0.043
Pairwise test	Pm1B-Pm1E	1.65	0.236	1.62	0.13
Pairwise test	Pm3B-Pm3E	3.98	**0.004**	5.50	**0.001**
Pairwise test	Pm1B-Pm3B	8.78	**0.004**	14.71	**0.001**
Pairwise test	Pm1E-Pm3E	4.81	**0.004**	6.1	**0.002**

except for Pm1B and Pm1E (Table 2). The principal coordinates analysis showed that species is the most important grouping factor (Fig. 7). Within each species, Pm1 showed high intraspecific variability in both food treatments, while intraspecific variability for Pm3 was much lower in the treatment where they were offered a bacterial mix. Homogeneity of dispersions was not achieved ($P > 0.05$) for factor species, reflecting the high variation within Pm1.

The core microbiome of specimens from the food experiment. Similar to the results of the field specimens, the fraction of OTUs shared between all specimens was very low. In total, 41 OTUs were shared between all 46 samples of the food experiment. The core of the Pm1 bacterial mixture treatment had 157 OTUs and the Pm3 bacterial mixture treatment had 261 core OTUs. The number of core OTUs was lower for the *E. coli* treatment: 85 core OTUs were present in Pm1 and 178 for Pm3. The core of all 20 Pm3 individuals contained 77 OTUs, while Pm1 had 52 OTUs shared among all 20 specimens. PERMANOVA on UniFrac distances showed that food (pseudo-$F_{1,39} = 3.59$, $P = 0.008$), species (pseudo-$F_{1,39} = 16.56$, $P = 0.001$) and the interaction food*species (pseudo-$F_{1,39} = 2.46$, $P = 0.043$) were significant. All pairwise comparisons were significant, except for the two food treatments of Pm1 (Table 2).

Biomarker taxa of specimens from the food experiment. For Pm1, 433 OTUs were identified as biomarkers, while 208 OTUs were identified as biomarker for Pm3. Taxonomic assignment of many OTUs was only achieved at the class level and 52 OTUs of the Pm3 biomarker taxa had no taxonomic assignment at all (Appendix S11, Supporting information). The biomarker OTUs that were identified up to family level belonged to the Flavobacteriaceae, Rhodobacteraceae, Alteromonadaceae, Pseudoalteromonadaceae and Vibrionaceae for both species, with an additional two families for the biomarker taxa of Pm1 (Phyllobacteriaceae and one unidentified family of the ordo Saprospirales). The complete list of biomarker OTUs for Pm1 and Pm3 with their taxonomic assignment can be found in Appendix S11 (Supporting information).

SEM and light microscope pictures. Scanning electron microscopy pictures revealed that the cuticle of the cryptic nematode species contained only very few bacteria, which were mainly located in the mid body region for the females, and in the tail region for the males (see Appendix S12, Supporting information). The morphology of the attached bacteria was quite uniform, suggesting a very low taxonomic diversity of the epibionts. The digital pictures that were taken from the sequenced specimens seconds before transferring them into the WLB further support that the bacterial densities and diversity on the cuticle of the three rhabditid nematodes were low.

Discussion

The nematode microbiome is highly diverse and species-specific

Our data show that the bacterial community associated with the *Litoditis* specimens contains at least 85 OTUs for the field specimens (Appendix S3, Supporting information). Most OTUs were present in very low frequency. Even under laboratory conditions and with *E. coli* as a food source, a high diversity was associated with the nematode specimens (lowest number: 1118 OTUs; Appendix S8, Supporting information). Applying the MiSeq protocol to the field specimens would very likely result in an even higher diversity than observed in the laboratory specimens. The microbiomes of the field specimens and cultured nematodes are not directly comparable because two different sequencing platforms (454 vs. Illumina platforms) and primer sets were used to generate sequence data which may introduce taxonomic and technical biases in terms of the microbial community recovered.

Despite the high number of bacterial OTUs associated with the field nematode specimens, only 2–6 OTUs were found in all six specimens of a particular species, and not a single OTU was found in all 18 specimens

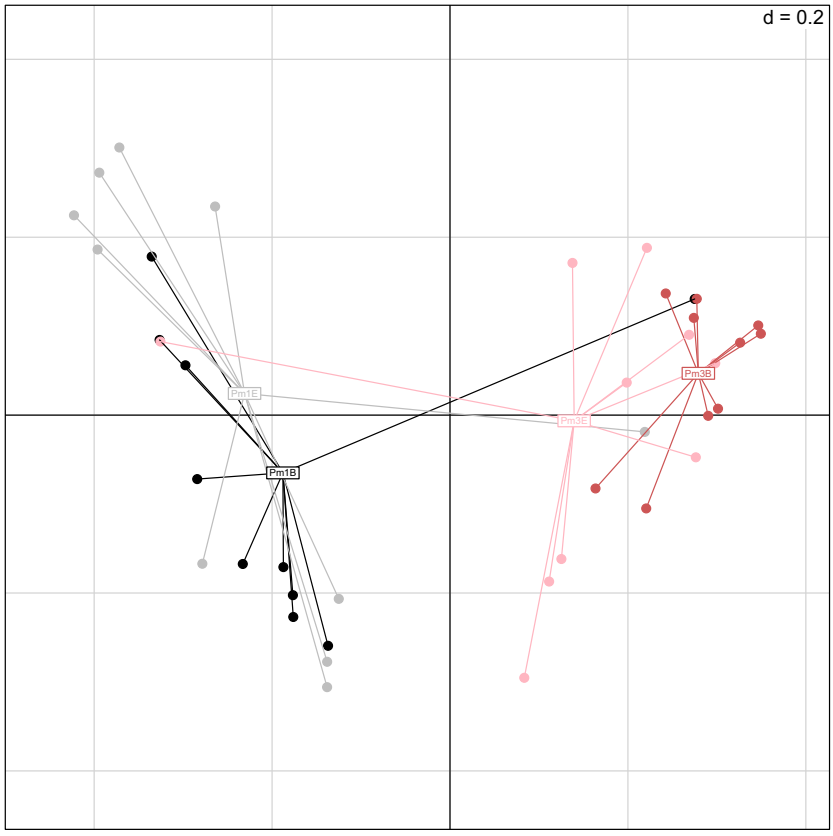

Fig. 7 Principal coordinates analysis plot of the generalized UniFrac distances for the two species (Pm1 black/grey and Pm3 red/pink) and the two food treatments. E = *E. coli* (grey/pink) and B = bacterial mixture (black/red).

(see Appendix S7, Supporting information). This was also true for the food experiment, in which 52 OTUs were shared among the 20 Pm1 specimens and 77 OTUs were shared among the 20 Pm3 specimens. The frequency of the core microbiome was very low, and although six core OTUs obtained a frequency higher than 1% in the rarefied data set, their abundance varied substantially between individuals (Fig. 5). Bacterial strains that are present in the core microbiome of a particular nematode species and that are absent in the other species can potentially confer an adaptation to the environment for that particular nematode species. Moreover, if such core OTUs are also present in the other nematode species than the species for which it is a core OTU, its abundance should be significantly different between nematode species. In other words, it would be identified as biomarker in the LeFSe analysis. Three core OTUs of Pm3 were completely absent in Pm1 when clustering at 97% for the reverse data set (Appendix S7, Supporting information): OTU310003 (Caulobacteraceae), OTU720489 (*Acinetobacter*) and OTU4449456 (*Acinetobacter*). They may thus be involved in mediating different tolerances to environmental conditions for Pm1 and Pm3. Two of these Pm3 core OTUs were also present in Pm2 (OTU310003 and OTU4449456) and were identified as biomarkers for Pm3 by the LeFSe analysis, suggesting that members of Caulobacteraceae and *Acinetobacter* may be involved in differential abiotic tolerances for Pm3. All Pm2 core OTUs were present in the two other species, and only one was identified as a biomarker for Pm2: OTU200979 (*Microbacterium*). This OTU may thus potentially be involved in generating tolerance to abiotic conditions for Pm2. Laboratory experiments show that Pm1 performs less well at higher temperatures, while population development of Pm3 was lower at lower temperatures (De Meester *et al.* 2015b). This corresponds with the prevalence of Pm3 during warmer seasons and to its near-absence during colder seasons (Derycke *et al.* 2006). Pm2 has a pan European distribution and appears to be a generalist as it is found in habitats that differ substantially in temperature and salinity (Derycke *et al.* 2008b). The microbiome '*sensu stricto*' may perform a critical role in the physiological adaptations to such environmental changes.

Sympatric, cryptic nematode species show differences in resource use

We hypothesized that the differences in the microbiomes '*sensu lato*' between the nematode species were linked to differential resource use, as all three species

are bacterivorous. We expected to find many more OTUs in the worms that had been feeding on the bacterial mix compared to those that had been fed *E. coli*. This appeared not to be the case, but there was a significant food effect (Table 2) on the microbiome, indicating that bacteria were differentially consumed by the worms in the two food treatments. The similar number of OTUs observed in both food treatments may indicate that the worms only fed on a small number of OTUs present in the bacterial mix. Yet, the taxonomic composition of the worms fed on the bacterial mix was quite diverse and resembled the one of the bacterial mix. The stock cultures of both worms contained a large number of OTUs (1996 and 1301 for Pm1 and Pm3, respectively; Appendix S8, Supporting information) indicating that the microbiome *sensu stricto* is highly diverse and that several bacterial strains of this microbiome are able to grow on the agar. The Pm1 and Pm3 microbiomes from the *E. coli* treatment shared 1271 and 1135 OTUs with the Pm1 and Pm3 culture microbiome, respectively. Consequently, the potential food of the worms in the *E. coli* treatment was probably as diverse as the bacterial mix (which contained 2496 OTUs vs. 552 OTUs for the *E. coli* suspension; Appendix S8, Supporting information). OTUs showing higher abundances in the cultures did not result in a higher abundance in the microbiome and vice versa. Moreover, the microbiomes of specimens fed with *E. coli* resembled the one of the stock cultures, and their intestinal colour clearly indicated that they were actively feeding to a similar extent as the specimens in the bacterial mix treatment, adding support to the idea that the worms in the *E. coli* treatments had a much more diverse food source than anticipated. Surprisingly, we did not find an increase of Enterobacteriaceae in the specimens fed *E. coli*. Yet, the *E. coli* suspension was clearly dominated by Enterobacteriaceae (Fig. 6B), providing evidence that our methodological approach was able to identify the *E. coli* sequences. The *E. coli* source consisted of frozen-and-thawed *E. coli* cells, and provided as such a 'soup' rich of nutrients instead of metabolically active cells. Add-back experiments have demonstrated that *C. elegans* requires metabolically active cells for normal development and fecundity (Lenaerts *et al.* 2008). Tracer experiments with *Litoditis* showed that radioactive labels were only present in the worms when fed labelled (unidentified) bacteria, while such a radioactive signal was absent when the worms were offered the growth medium of that same bacterial mix without cells despite the fact that this medium was much more heavily labelled than the bacterial cells (Moens, unpublished data). This suggests that the nutrient rich 'soup' provided by the *E. coli* suspension can stimulate extensive growth of other bacteria from the worm microbiome and that the soup itself was not ingested by the worms.

The food experiment further showed that the microbiome of Pm1 did not differ according to food type, while that of Pm3 did. This result can be explained by two nonmutually exclusive scenarios: (i) the Pm3 microbiome '*sensu stricto*' (Pm3E) differs considerably from the bacterial mixture while the Pm1 microbiome '*sensu stricto*' (Pm1E) is similar to the bacterial mixture. Feeding of Pm3 on the bacterial mix would then lead to significant differences between Pm3E-Pm3B but not between Pm1E-Pm1B. Comparison of the number of OTUs shared between the *E. coli* fed specimens and the bacterial mix does not support this hypothesis, as Pm3 specimens typically show a higher number of shared OTUs with the bacterial mix than Pm1 specimens (Appendix S13, Supporting information); (ii) the two species show different feeding behaviours with Pm3 feeding more selectively on a smaller portion of the bacterial mixture, while Pm1 feeds on a much wider range of bacterial strains from the mixture. This hypothesis is supported by the larger variability between individual Pm1 specimens that were fed the bacterial mix compared to the much smaller interindividual variability in Pm3 (PCoA plot, Fig. 7) and by the higher number of biomarker taxa identified in Pm1 compared to Pm3 (Appendix S11, Supporting information), indicating that Pm3 is a much more selective feeder than Pm1. We also found a significant species effect (Table 2), suggesting that Pm1 and Pm3 were feeding on different bacterial species. As the Pm1 and Pm3 nematodes from the food experiment have been kept for several generations under controlled abiotic conditions, the biomarker taxa revealed by the LeFSe analysis are likely linked to differential resource use of the two species. The individual differences in bacterial diet cannot be linked to particular life stages or certain ecological morphs as we only selected adult specimens for our population genetic analysis (Derycke *et al.* 2006). Observations on the feeding behaviour of living *L. marina* specimens showed that the size of the prey forms an important filter for ingestion (Moens & Vincx 1997; Tietjen & Lee 1975), and the buccal cavity of Pm3 specimens is smaller than that of Pm1 specimens (Derycke *et al.* 2008a) suggesting that size selection may be one aspect contributing to differences in selectivity. We cannot exclude that the four OTUs potentially involved in adaptation to abiotic conditions are linked to resource use, but *Microbacterium* was present in all three nematode species, and also different *Acinetobacter* OTUs were found in all three nematode species, suggesting that these types of bacterial strains can be ingested by all three species and that size selection through feeding may not be an important mechanism to explain the different abundances of these

core OTUs. Instead, the high variability among individuals implies that there are constraints in resource use that prevent individuals from using the whole range of available resources. These constraints may act at the individual level (e.g. uptake ability, morphology, behaviour), but probably more so at the population level, where high intraspecific competition can increase individual niche specialization (Svanback & Bolnick 2007). Intraspecific competition has been observed in all three species (De Meester *et al.* 2015a) and individual niche specialization can increase the niche breadth of the total population (Bolnick *et al.* 2007). This agrees well with the high diversity of the microbiomes observed in each of the three species, and can affect interspecific interactions, as niche overlap between species is likely to increase with increased niche width.

Niche partitioning between cryptic species can partially explain their coexistence

The nematode microbiomes were dominated by Alphaproteobacteria and Gammaproteobacteria, Bacteroidetes and Verrucomicrobia which are the dominant groups found on *Fucus vesiculosus* (Lachnit *et al.* 2011), the habitat from which the nematode specimens were isolated. The microbiomes of Pm1 and Pm3 from the field were clearly different from each other, and the food experiment shows that these differences are linked both to the feeding activity of the species but also to the presence of a nematode species-specific microbiome. Pm1 and Pm3 specimens more often co-occur in the field than Pm1 with Pm2 or than Pm3 with Pm2 (Appendix S1, Supporting information). These data agree well with the ecological theory of resource partitioning, where species can coexist when they are using different resources (MacArthur & Levins 1967). However, if resource partitioning would be the only driver for coexistence of these cryptic species, we would expect to find Pm1 coexisting with Pm3 throughout the year, which is not the case (Derycke *et al.* 2006). Coexistence of species is also governed by their common responses to environmental changes (Chesson 2000; Leibold & McPeek 2006) and the microbiome may perform a critical role in the physiological adaptations to such environmental changes and hence in the fitness of the nematode hosts. Dedicated attempts (using repeated transfer of worms through mixtures of antibiotics and even incorporating antibiotics in the stock culture media for several subsequent generations) at removing bacteria other than the *E. coli* supplied as food failed (P. Gilarte, unpublished data), suggesting a tight association between nematodes and (components of) their microbiomes. Fitness differences imply that differential responses to abiotic environmental variability can also have stabilizing effects on the coexistence between cryptic nematode species. In addition to these deterministic variations in environment, the ephemeral nature of the *Fucus* habitat on which the species live induces strong stochastic variability in the environment. The coexistence of Pm1 and Pm3 is therefore likely to be determined by both resource partitioning and differential responses to abiotic changes. Although microbiome differentiation was less straightforward between Pm1 and Pm2, phylogeographic data revealed that Pm2 has a more widespread distribution than the two other species, suggesting it has a broader 'abiotic' niche than the other species. The microbiome of Pm2 was also not differentiated from either of the two other species.

Methodological considerations

Our understanding of the degree of resource selectivity in nematode feeding behaviour is generally very poor: several laboratory experiments have demonstrated a high capacity to select among even very similar food items (Moens *et al.* 1999), but reliable approaches to study such detailed resource selectivity under more natural conditions have been lacking. Moreover, stable isotope and other approaches which measure food absorption usually require pooling of individuals for a single analysis (Carman & Fry 2002). Our approach complements others, but provides a substantial advance compared to any previous work on resource utilization of free-living nematodes or other microscopic eukaryotes by characterizing the complete bacterial community of individual specimens of three nematode species. The marker gene survey approach used here allows to assess selective feeding behaviour of single nematode specimens, which has not been possible with methods widely used to assess resource use (e.g. stable isotope analysis). However, our results also show the presence of a highly diverse endosymbiont community that differs substantially among individuals. Our morphological investigation of the bacteria on the cuticula detected only few bacterial morphotypes suggesting that most of the microbiome is located inside the body of the worm (see Appendix S12, Supporting information).

Conclusion

The natural bacterial communities of sympatrically distributed cryptic nematode species are highly diverse and show pronounced intraspecific diversity. The species-specific microbiomes may play a role in the different tolerances of the nematode species to abiotic conditions. Importantly, the differences in selective feeding of morphologically similar nematode species may have a cascading effect on the microbial commu-

nity and on the functioning of the whole decomposition system, as alterations in microbial communities can alter mineralization of organic matter (Nascimento *et al.* 2012). Consequently, cryptic diversity may have hitherto unpredicted consequences for biodiversity–ecosystem functioning relationships in the marine benthos

Acknowledgements

We gratefully acknowledge John Gaspar for his help in denoising the 454 GS FLX sequence data and Marjolein Couvreur for generating the SEM pictures. S.D. is funded by the Belgian Science Policy Office (Belspo). This research was financially supported through the F.W.O. projects 3G019209 and 3G038715, and by Ghent University through the BOF project 01GA1911W. We are thankful for the valuable comments of three anonymous referees which greatly improved a previous version of this manuscript.

References

Bickford D, Lohman DJ, Sodhi NS, *et al.* (2007) Cryptic species as a window on diversity and conservation. *Trends in Ecology & Evolution*, **22**, 148–155.

Bolnick DI, Svanback R, Araujo MS, Persson L (2007) Comparative support for the niche variation hypothesis that more generalized populations also are more heterogeneous. *Proceedings of the National Academy of Sciences of the United States of America*, **104**, 10075–10079.

Cabreiro F, Gems D (2013) Worms need microbes too: microbiota, health and aging in Caenorhabditis elegans. *EMBO Molecular Medicine*, **5**, 1300–1310.

Caporaso JG, Kuczynski J, Stombaugh J, *et al.* (2010) QIIME allows analysis of high-throughput community sequencing data. *Nature Methods*, **7**, 335–336.

Caporaso JG, Lauber CL, Walters WA, *et al.* (2012) Ultra-high-throughput microbial community analysis on the Illumina HiSeq and MiSeq platforms. *Isme Journal*, **6**, 1621–1624.

Carman KR, Fry B (2002) Small-sample methods for delta C-13 and delta N-15 analysis of the diets of marsh meiofaunal species using natural-abundance and tracer-addition isotope techniques. *Marine Ecology Progress Series*, **240**, 85–92.

Chen J, Bittinger K, Charlson ES, *et al.* (2012) Associating microbiome composition with environmental covariates using generalized UniFrac distances. *Bioinformatics*, **28**, 2106–2113.

Chesson P (2000) Mechanisms of maintenance of species diversity. *Annual Review of Ecology and Systematics*, **31**, 343 +.

De Meester N, Derycke S, Bonte D, Moens T (2011) Salinity effects on the coexistence of cryptic species: A case study on marine nematodes. *Marine Biology*, **158**, 2717–2726.

De Meester N, Derycke S, Moens T (2012) Differences in time until dispersal between cryptic species of a marine nematode species complex. *PLoS ONE*, **7**, e42674.

De Meester N, Derycke S, Rigaux A, Moens T (2015a) Active dispersal is differentially affected by inter- and intraspecific competition in closely related nematode species. *Oikos*, **124**, 561–570.

De Meester N, Derycke S, Rigaux A, Moens T (2015b) Temperature and salinity induce differential responses in life histories of cryptic nematode species. *Journal of Experimental Marine Biology and Ecology*, **472**, 54–62.

Derycke S, Remerie T, Vierstraete A, *et al.* (2005) Mitochondrial DNA variation and cryptic speciation within the free-living marine nematode *Pellioditis marina*. *Marine Ecology Progress Series*, **300**, 91–103.

Derycke S, Backeljau T, Vlaeminck C, *et al.* (2006) Seasonal dynamics of population genetic structure in cryptic taxa of the *Pellioditis marina* complex (Nematoda: Rhabditida). *Genetica*, **128**, 307–321.

Derycke S, Fonseca G, Vierstraete A, *et al.* (2008a) Disentangling taxonomy within the *Rhabditis (Pellioditis) marina* (Nematoda, Rhabditidae) species complex using molecular and morphological tools. *Zoological Journal of the Linnean Society*, **152**, 1–15.

Derycke S, Remerie T, Backeljau T, *et al.* (2008b) Phylogeography of the *Rhabditis (Pellioditis) marina* species complex: evidence for long-distance dispersal, and for range expansions and restricted gene flow in the northeast Atlantic. *Molecular Ecology*, **17**, 3306–3322.

Derycke S, Backeljau T, Moens T (2013) Dispersal and gene flow in free-living marine nematodes. *Frontiers in Zoology*, **10**, 000–000.

Edgar RC, Haas BJ, Clemente JC, Quince C, Knight R (2011) UCHIME improves sensitivity and speed of chimera detection. *Bioinformatics*, **27**, 2194–2200.

Elmer KR, Bonett RM, Wake DB, Lougheed SC (2013) Early Miocene origin and cryptic diversification of South American salamanders. *BMC Evolutionary Biology*, **13**, 000–000.

Estifanos TK, Traunspurger W, Peters L (2013) Selective feeding in nematodes: a stable isotope analysis of bacteria and algae as food sources for free-living nematodes. *Nematology*, **15**, 1–13.

Fonseca G, Derycke S, Moens T (2008) Integrative taxonomy in two free-living nematode species complexes. *Biological Journal of the Linnean Society*, **94**, 737–753.

Fonseca VG, Carvalho GR, Sung W, *et al.* (2010) Second-generation environmental sequencing unmasks marine metazoan biodiversity. *Nature Communications*, **1**, 000–0000.

Gaspar JM, Thomas WK (2015) FlowClus: efficiently filtering and denoising pyrosequenced amplicons. *BMC Bioinformatics*, **16**, 000–0000.

Gilbert JA, Jansson JK, Knight R (2014) The Earth Microbiome project: successes and aspirations. *BMC Biology*, **12**, 69.

Gingold R, Ibarra-Obando SE, Rocha-Olivares A (2011) Spatial aggregation patterns of free-living marine nematodes in contrasting sandy beach micro-habitats. *Journal of the Marine Biological Association of the United Kingdom*, **91**, 615–622.

Glasby CJ, Wei NWV, Gibb KS (2013) Cryptic species of Nereididae (Annelida: Polychaeta) on Australian coral reefs. *Invertebrate Systematics*, **27**, 245–264.

Heip C, Vincx M, Vranken G (1985) The ecology of marine nematodes. *Oceanography and Marine Biology: an Annual Review*, **23**, 399–489.

Inglis W, Coles J (1961) The species of *Rhabditis* (Nematoda) found in rotting seaweed on British beaches. *Bulletin of the British Museum of Natural History (Zoology)*, **7**, 320–333.

Knowlton N (1993) Sibling species in the sea. *Annual Review of Ecology and Systematics*, **24**, 189–216.

Lachnit T, Meske D, Wahl M, Harder T, Schmitz R (2011) Epibacterial community patterns on marine macroalgae are

host-specific but temporally variable. *Environmental Microbiology*, **13**, 655–665.
Leibold MA, McPeek MA (2006) Coexistence of the niche and neutral perspectives in community ecology. *Ecology*, **87**, 1399–1410.
Lenaerts I, Walker G, Van Hoorebeke L, Gems D, Vanfleteren J (2008) Dietary restriction of *Caenorhabditis elegans* by axenic culture reflects nutritional requirement for constituents provided by metabolically active microbes. *Journals of Gerontology Series A Biological Sciences and Medical Sciences*, **63**, 242–252.
de Leon GPP, Nadler SA (2010) What we don't recognize can hurt us: a plea for awareness about cryptic species. *Journal of Parasitology*, **96**, 453–464.
MacArthur R, Levins R (1967) The limiting similarity, convergence, and divergence of coexisting species. *American Naturalist*, **101**, 377–385.
Martin M (2011) Cutadapt removes adapter sequences from high-throughput sequencing reads. *EMBnet. Journal*, **17**, 10–12.
Moens T, Vincx M (1997) Observations on the feeding ecology of estuarine nematodes. *Journal of the Marine Biological Association of the United Kingdom*, **77**, 211–227.
Moens T, Vincx M (1998) On the cultivation of free-living marine and estuarine nematodes. *Helgoland Marine Research*, **52**, 115–139.
Moens T, Verbeeck L, de Maeyer A, Swings J, Vincx M (1999) Selective attraction of marine bacterivorous nematodes to their bacterial food. *Marine Ecology-Progress Series*, **176**, 165–178.
Nascimento FJA, Naslund J, Elmgren R (2012) Meiofauna enhances organic matter mineralization in soft sediment ecosystems. *Limnology and Oceanography*, **57**, 338–346.
Perez-Portela R, Almada V, Turon X (2013) Cryptic speciation and genetic structure of widely distributed brittle stars (Ophiuroidea) in Europe. *Zoologica Scripta*, **42**, 151–169.
Pfenninger M, Schwenk K (2007) Cryptic animal species are homogeneously distributed among taxa and biogeographical regions. *BMC Evolutionary Biology*, **7**, 121.
Ristau K, Steinfartz S, Traunspurger W (2013) First evidence of cryptic species diversity and significant population structure in a widespread freshwater nematode morphospecies (Tobrilus gracilis). *Molecular Ecology*, **22**, 4562–4575.
Segata N, Izard J, Waldron L, *et al.* (2011) Metagenomic biomarker discovery and explanation. *Genome Biology*, **12**, R60.
Seymour MK, Wright KA, Doncaster CC (1983) The action of the anterior feeding apparatus of *Caenorhabditis elegans* (Nematoda, Rhabditida). *Journal of Zoology*, **201**, 527–539.
Sison-Mangus MP, Jiang S, Tran KN, Kudela RM (2014) Host-specific adaptation governs the interaction of the marine diatom, Pseudo-nitzschia and their microbiota. *ISME Journal*, **8**, 63–76.
Steyaert M, Garner N, van Gansbeke D, Vincx M (1999) Nematode communities from the North Sea: environmental controls on species diversity and vertical distribution within the sediment. *Journal of the Marine Biological Association of the United Kingdom*, **79**, 253–264.
Sudhaus W, Kiontke K (2007) Comparison of the cryptic nematode species *Caenorhabditis brenneri* sp n. and *C. remanei* (Nematoda: Rhabditidae) with the stem species pattern of the *Caenorhabditis elegans* group. *Zootaxa*, **1456**, 45–62.
Svanback R, Bolnick DI (2007) Intraspecific competition drives increased resource use diversity within a natural population. *Proceedings of the Royal Society B-Biological Sciences*, **274**, 839–844.
Team RDC (2008) *R: A Language and Environment for Statistical Computing*. R Foundation for Statistical Computing, Vienna, Austria.
Tietjen JH, Lee JJ (1975) Axenic culture and uptake of dissolved organic substances by the marine nematode, *Rhabditis marina* Bastian. *Cahiers de Biologie Marine*, **XVI**, 685–693.
Vanaverbeke J, Gheskiere T, Vincx M (2000) The meiobenthos of subtidal sandbanks on the Belgian Continental Shelf (Southern Bight of the North Sea). *Estuarine Coastal and Shelf Science*, **51**, 637–649.
Wieser W (1953) Die Beziehung zwischen Mundhöhlengestalt, Ernährungsweise und Vorkommen bei freilebenden marinen Nematoden. *Arkiv för Zoologi*, **4**, 439–484.
Zhang J, Kobert K, Flouri T, Stamatakis A (2014) PEAR: a fast and accurate Illumina Paired-End reAd mergeR. *Bioinformatics*, **30**, 614–620.
Zoetendal EG, Akkermans ADL, De Vos WM (1998) Temperature gradient gel electrophoresis analysis of 16S rRNA from human fecal samples reveals stable and host-specific communities of active bacteria. *Applied and Environmental Microbiology*, **64**, 3854–3859.

S.D. collected and analysed the 454 data and wrote the manuscript; N.D.M. performed the food experiment and analysed the MiSeq data; A.R. performed the molecular analyses; W.K.T. conceived the study and along with S.C. and H.B. outlined opportunities to investigate meiobenthic diets using amplicon sequencing; T.M. and N.D.M. critically revised the manuscript; and all authors contributed to the final version of the manuscript.

Data accessibility

The raw sequence data of the two runs on the 454 GS FLX system are available in the Short Read Archive at NCBI under accession no. SRP064694. The raw sequences of the MiSeq run are available under accession no. SRP064727.

Supporting information

Additional supporting information may be found in the online version of this article.

Appendix S1 Field distribution of four cryptic *Litoditis marina* species (Pm1, Pm2, Pm3 and Pm4) in the Scheldt estuary in the Netherlands in four consecutive seasons. Figure adapted from Derycke *et al.* (2006).

Appendix S2 Primer sequences used to amplify the 16S rRNA gene of 18 *Litoditis marina* specimens in two runs on one-eighth

of a plate of the 454 GS FLX Titanium system. Adaptor, MID tag and primer sequences for the forward and reverse data sets are given.

Appendix S3 Summary of the sequence data from the two 454 runs performed on 18 field specimens.

Appendix S4 Summary of the analyses to investigate variability between the technical replicates.

Appendix S5 Figures related to alpha-diversity and beta-diversity measurements of the forward data set generated using the 454 platform of the field specimens.

Appendix S6 Rank abundance plots of the forward and reverse data sets generated with the 454 platform of the field specimens.

Appendix S7 The core OTUs of the forward and reverse data sets that are present in 100% of the specimens of species Pm1, Pm2 and Pm3 from the field. OTUs identified with LeFSe are indicated in bold. For the reverse data set, OTUs were generated using 97% and 99% similarity.

Appendix S8 Summary of the sequence data from the MiSeq run on the specimens of the food experiment. Summary of the sequence data from a separate MiSeq run containing three biological replicas of the *E. coli* suspension are also provided.

Appendix S9 Detailed description of the taxonomic composition at the phylum, class and family level for the specimens of the food experiment.

Appendix S10 Graphs of alpha diversity (rarefaction curves of number of OTUs and Shannon index, rank abundance plots) of the specimens of the food experiment.

Appendix S11 List of biomarker taxa identified by LeFSe for Pm1 and Pm3 from the food experiment. OTU ID and taxonomic assignment using Greengenes are included.

Appendix S12 SEM pictures of nematode specimens from Pm1, Pm2 and Pm3 with bacteria attached to the cuticula.

Appendix S13 Number of shared OTUs between each nematode specimen and each replica of the bacterial mix.

Appendix S14 Table with OTU IDs from the forward (sheet 1) and reverse data set (sheet 2) for the field specimens, along with their frequency in each specimen, the taxonomic assignment using Uclust or Blast, and the quality score of the taxonomic assignment.

Appendix S15 Fasta file with representative sequences of OTUs from the forward data set from the field specimens.

Appendix S16 Fasta file with representative sequences of OTUs from the reverse data set from the field specimens.

Appendix S17 Table with OTU IDs from the MiSeq data set for the specimens of the food experiment, along with their frequency in each specimen, the taxonomic assignment using Uclust, and the quality score of the taxonomic assignment.

Appendix S18 Fasta file with representative sequences from OTUs from the MiSeq run for the specimens of the food experiment.